

# Use of $^{18}\text{O}$ Labels to Monitor Deamidation during Protein and Peptide Sample Processing

Xiaojuan Li,<sup>a</sup> Jason J. Cournoyer,<sup>b</sup> Cheng Lin,<sup>a</sup> and Peter B. O'Connor<sup>a</sup>

<sup>a</sup> Mass Spectrometry Resource, Department of Biochemistry, Boston University School of Medicine, Boston, Massachusetts, USA

<sup>b</sup> Department of Chemistry, Boston University, Boston, Massachusetts, USA

Nonenzymatic deamidation of asparagine residues in proteins generates aspartyl (Asp) and isoaspartyl (isoAsp) residues via a succinimide intermediate in a neutral or basic environment. Electron capture dissociation (ECD) can differentiate and quantify the relative abundance of these isomeric products in the deamidated proteins. This method requires the proteins to be digested, usually by trypsin, into peptides that are amenable to ECD. ECD of these peptides can produce diagnostic ions for each isomer; the  $c + 58$  and  $z - 57$  fragment ions for the isoAsp residue and the fragment ion  $((M + nH)^{(n-1)+} - 60)$  corresponding to the side-chain loss from the Asp residue. However, deamidation can also occur as an artifact during sample preparation, particularly when using typical tryptic digestion protocols. With  $^{18}\text{O}$  labeling, it is possible to differentiate deamidation occurring during trypsin digestion which causes a +3 Da ( $^{18}\text{O}_1 + 1\text{D}$ ) mass shift from the pre-existing deamidation, which leads to a +1-Da mass shift. This paper demonstrates the use of  $^{18}\text{O}$  labeling to monitor three rapidly deamidating peptides released from proteins (calmodulin, ribonuclease A, and lysozyme) during the time course of trypsin digestion processes, and shows that the fast (~4 h) trypsin digestion process generates no additional detectable peptide deamidations. (J Am Soc Mass Spectrom 2008, 19, 855–864) © 2008 American Society for Mass Spectrometry

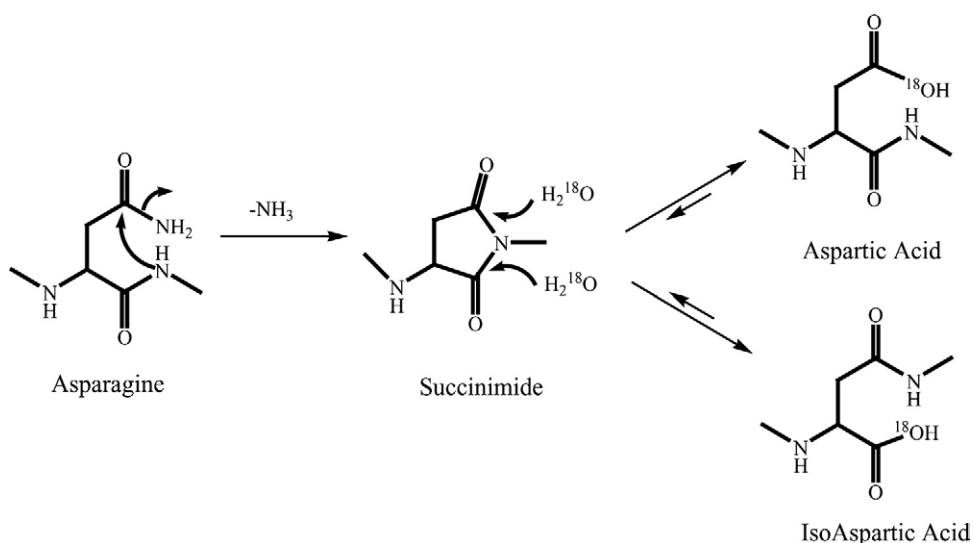
Deamidation is a spontaneous nonenzymatic post-translational modification of proteins. It plays an important role in protein degradation and is postulated to function as a timer in aging [1–4]. Deamidation occurs on asparagine (Asn) and glutamine (Gln) residues and has been observed and characterized in a wide variety of proteins both in vivo and in vitro. The Asn deamidation takes place much more rapidly than that of Gln (up to ten times faster), because the formation of a six-membered cyclic imide is entropically less favorable [5, 6]. Upon deamidation, the asparaginyl residue is converted to a mixture of isoaspartyl (isoAsp) and aspartyl (Asp) residues.

Many factors can influence deamidation rates, such as protein sequence [5, 7, 8], secondary structure [9], local three-dimensional structure [10], pH, temperature, ionic strength, buffer ions, turnover of the protein, and other solution properties [11, 12]. In many cases, the deamidation rate is influenced by the primary structure. It is well known that Gly or Ser located on the C-terminal side of Asn greatly accelerates Asn deamidation. Ser and, to a lesser extent, Thr and Lys preceding Asn (at its N-terminal side) can also facilitate the Asn deamidation [11, 12]. The small side chains of Gly and Ser allow extensive conformational changes, whereas amino acids with branched, bulky, hydrophobic side

chains or Asn/Gln located close to intramolecular disulfide bonds reduce the conformational flexibility necessary for the intermediate formation [5]. Furthermore, the secondary and tertiary structures usually determine whether deamidation actually occurs [6]. Stabilization of Asn residues by higher-order structures has been observed, which may result from conformational restrictions and the reduced nucleophilic reactivity of the backbone NH centers due to hydrogen bonding [9, 13]. Also, the structural change induced by one deamidation site may further influence the deamidation rates at other sites [5].

Deamidation may occur via two different pathways depending on the pH of the solution, which can affect the abundance of products. In an acidic solution (pH <5), deamidation proceeds via the acid-catalyzed pathway, where direct hydrolysis of the Asn residue side-chain amide group results in the formation of Asp as the only product. At pH >5, deamidation primarily occurs via a base-catalyzed pathway, in which the Asn residue is converted to a succinimide intermediate that can then hydrolyze rapidly to produce L-Asp and L-isoAsp, typically in a 1:3 ratio for random-coil peptides [8] (Scheme 1). This reaction is reversible in aqueous solution. The deamidation rate reaches a minimum at approximately pH of 5. In basic conditions, the rate-limiting step is the intramolecular nucleophilic attack on the side-chain carbonyl by the nitrogen. In acidic conditions, the rate-limiting

Address reprint requests to Dr. Peter B. O'Connor, Boston University School of Medicine, Mass Spectrometry Resource, Department of Biochemistry, 670 Albany St., Room 504, Boston, MA 02118. E-mail: [poconnor@bu.edu](mailto:poconnor@bu.edu)



**Scheme 1.** The mechanism of the asparagine residue deamidation in  $\text{H}_2^{18}\text{O}$ .

step is the direct elimination of  $\text{NH}_2^-$  from the tetrahedral intermediate [1, 12, 14, 15].

Methods for detection of deamidation are usually based on the charge-sensitive techniques or mass spectrometry analysis. Deamidation introduces negative charges to a protein that shifts its isoelectric point (pI). It also results in a +0.984-Da mass shift from Asn to Asp/isoAsp, which can be detected and the extent measured using the mass defect and the envelope deconvolution method [16–19]. The advantages of these techniques are that protein samples can be introduced into a Fourier transform mass spectrometer without sample pretreatment (e.g., digestion, separation, absorption, and ionization) and that protein deamidation can be measured quantitatively without tandem mass spectrometry (MS/MS) analysis. Although determining the conversion of Asn to Asp/isoAsp is relatively straightforward, distinguishing the products Asp and isoAsp is more challenging. Several methods for the Asp/isoAsp differentiation exist, including NMR [20], HPLC [21], Edman-based sequencing [22], and antibody detection [23], although they all have certain limitations: the former three typically require relatively large quantity of proteins and the latter requires highly specific antibodies.

MS/MS methods can facilitate the detection and quantification of deamidation while only requiring femtomolar to picomolar amount of samples. In addition, they can also provide very specific information on the deamidation sites and help differentiate and quantify the ratio of the Asp and isoAsp products. In collisionally activated dissociation (CAD), the two isomers have different, identifiable side-chain fragmentation patterns for the N- and C-terminal ions [22, 24, 25]. In electron capture dissociation (ECD) [26–29] and electron-transfer dissociation (ETD) [30, 31], their fragmentations also produce different diagnostic ions: the  $[(M + nH)^{(n-1)+} - 60]$  fragment ion for the detection of the Asp, and the  $c \cdot + 58$  and  $z - 57$

ions for the detection and location of the isoAsp [32–35]. However, ECD of intact proteins is often inefficient because the number of available fragmentation channels is large and the resulting fragments frequently remain bound by noncovalent interactions and are thus undetectable. In most cases, the proteins need to be digested to form small peptides, most commonly by trypsin, before they are tested [36]. Trypsin digestion, which usually occurs at pH of about 8 and results in many small random coil peptides, is well known to accelerate base-mediated deamidation. Thus, it is important to distinguish the artifactual deamidations introduced during the sample processing steps from those that have occurred naturally to decrease the uncertainty about the biological relevance of any observed modifications.

One common method to monitor artificial, spontaneous reactions in mass spectrometry is to incorporate stable isotopic mass labels. For example, proteolytic  $^{18}\text{O}$  labeling and hydrogen/deuterium exchange have been used extensively in studies of protein modification, such as comparative proteomics [37–40], quantitative proteomics [41], protein conformational studies [42], protein dynamics analysis [43], protein–ligand interactions [44], and protein aggregates research [45, 46]. Proteolytic  $^{18}\text{O}$  labeling, in particular, has been used in the identification and quantification of succinimide [47] and citrullination [48] in proteins. The mechanism of protease catalyzed incorporation of  $^{18}\text{O}$  into peptide fragments has been studied extensively [49, 50]. For trypsin, it usually results in up to two  $^{18}\text{O}$  atoms incorporation into the peptide C-terminus, causing a mass shift of +2 Da per  $^{18}\text{O}$  substitution. Since deamidation involves hydrolysis, sample preparation procedures performed in  $\text{H}_2^{18}\text{O}$  will also offer the possibility of direct incorporation of a mass label during the reaction. If a peptide deamidates in  $\text{H}_2^{18}\text{O}$ , it not only gets the +0.984-Da mass shift from the deamidation reaction, but also incorporates an  $^{18}\text{O}$  atom on the

newly formed Asp/isoAsp residue to get a total mass shift of +2.988 Da. This paper demonstrates the use of this simple mass labeling procedure for distinguishing the artificial deamidation that occurred during the tryptic digestion process, which leads to a +3 Da mass shift, from the preexisting deamidation in the sample that causes a +1-Da mass shift. Furthermore, fragment ions containing the artificial deamidation site will also be 2 Da heavier than those containing the natural deamidation site, providing additional insight into the origin and location of the deamidation. Time course studies monitoring the extent of deamidations in three rapidly deamidating peptides released from tryptic digestions of proteins were also performed, which showed no detectable artificial deamidation during fast (~4 h) tryptic digestions at 37 °C and pH of about 8.3.

## Experimental

### Materials

Sequencing grade trypsin was purchased from Roche Applied Science (Indianapolis, IN). HPLC grade H<sub>2</sub><sup>16</sup>O was purchased from Honeywell/Burdick & Jackson (Muskegon, MI). All other chemicals, proteins, and H<sub>2</sub><sup>18</sup>O (95% <sup>18</sup>O) were purchased from Sigma (St. Louis, MO).

### Reduction and Alkylation

Ribonuclease A (RNase A) and lysozyme each have four disulfide bonds that were reduced and alkylated before analysis as described previously [33]. Briefly, proteins were reduced in 6 M urea/50 mM ammonium bicarbonate at pH 6, with tenfold molar excess of dithiothreitol over disulfide bonds and the resultant mixtures were incubated for 1 h at 37 °C. Iodoacetamide was then added in fivefold molar excess over cysteine residues and the resultant mixtures were incubated for 1 h in the dark at room temperature. The samples were dried and purified by home-made Poros 50 R1 packed solid-phase microextraction tip (Applied Biosystems, Foster City, CA). At each stage of sample processing, the sample was monitored by electrospray ionization Fourier-transform ion cyclotron resonance mass spectrometry (ESI FTICR-MS). The reduced and alkylated RNase A and lysozyme were then dried for use in the time course digestion.

### <sup>18</sup>O-Labeled Time Course Digestion

Calmodulin (20 μg), RNase A, and lysozyme (both 20 μg, denatured and purified) were each dissolved into 50 μL of 0.1 M ammonium bicarbonate buffer (pH 8.3) prepared using H<sub>2</sub><sup>18</sup>O. Trypsin (1 μg) was added to each solution, yielding a wt/wt ratio of 1:20, purged with N<sub>2</sub> gas, sealed, and incubated at 37 °C. Aliquots were taken at 2, 4, 6, 8, and 24 h, with an additional aliquot taken at 48 h for RNase A and lysozyme, due to their slower deamidation rates. Each aliquot was imme-

diately frozen at -80 °C to stop the reaction and washed later by an equal volume of H<sub>2</sub><sup>18</sup>O twice to desalt before mass spectrometry analysis.

### <sup>16</sup>O-Labeled Controls

Control experiments were done by using the same proteins and methods described earlier in the <sup>18</sup>O-labeled time course digestion section, except that H<sub>2</sub><sup>16</sup>O was used in place of H<sub>2</sub><sup>18</sup>O.

### Calmodulin <sup>18</sup>O-Labeled Triplicate Experiments

The digestion of 30 μg of calmodulin powder with 1.5 μg dried trypsin in 75 μL of 0.1 M ammonium bicarbonate buffer (pH 8.3) was performed in triplicate and incubated at 37 °C. Sample aliquots were taken according to the time course, frozen, washed, and analyzed as described earlier.

### Mass Spectrometry Analysis

ESI FTICR-MS was performed on a custom qQQ-FT-MS instrument equipped with an external nanospray ion source [51, 52]. ECD experiments used an indirectly heated dispenser cathode placed about 3 cm from the cell [53–55]. The control samples were electrosprayed at approximately 10<sup>-5</sup> M concentration in 49.5:49.5:1 of methanol:water:formic acid spray solution, whereas the <sup>18</sup>O-labeled samples were electrosprayed at the same concentration, but in 24.5:74.5:1 of methanol:water:formic acid spray solution. The different spray solution used was necessary to avoid ESI tip clogging, so that stable spray could be achieved for the <sup>18</sup>O-labeled samples. Multiply charged precursor ions were isolated using the front-end resolving quadrupole (Q1), followed by external accumulation in the CAD cell (Q2) before being transferred to the ICR cell and trapped by gated trapping. These ions were then irradiated with low-energy electrons (~0.2 eV) for time periods ranging from 50 to 120 ms to generate ECD fragments. A conventional FTMS excitation/detection sequence was used and the signal was averaged over 20 to 50 scans. All ECD spectra were internally calibrated and the peak lists are available in the supplementary data section.

## Results and Discussion

### Calmodulin Tryptic Peptide ESI FTMS Spectra (<sup>16</sup>O versus <sup>18</sup>O)

Figure 1 shows the mass spectra of the triply charged calmodulin tryptic peptide (<sup>91</sup>VFDKDGNGYISAAELR<sub>106</sub>) ion in a tryptic digestion time course study over 24 h in H<sub>2</sub><sup>16</sup>O and H<sub>2</sub><sup>18</sup>O. The inset shows the theoretical isotopic distribution of this peptide, which was calculated using the Yergey algorithm [59] as implemented in Isopro 3.0 (IonSource.com). Calmodulin is the primary cellular calcium receptor, which mediates

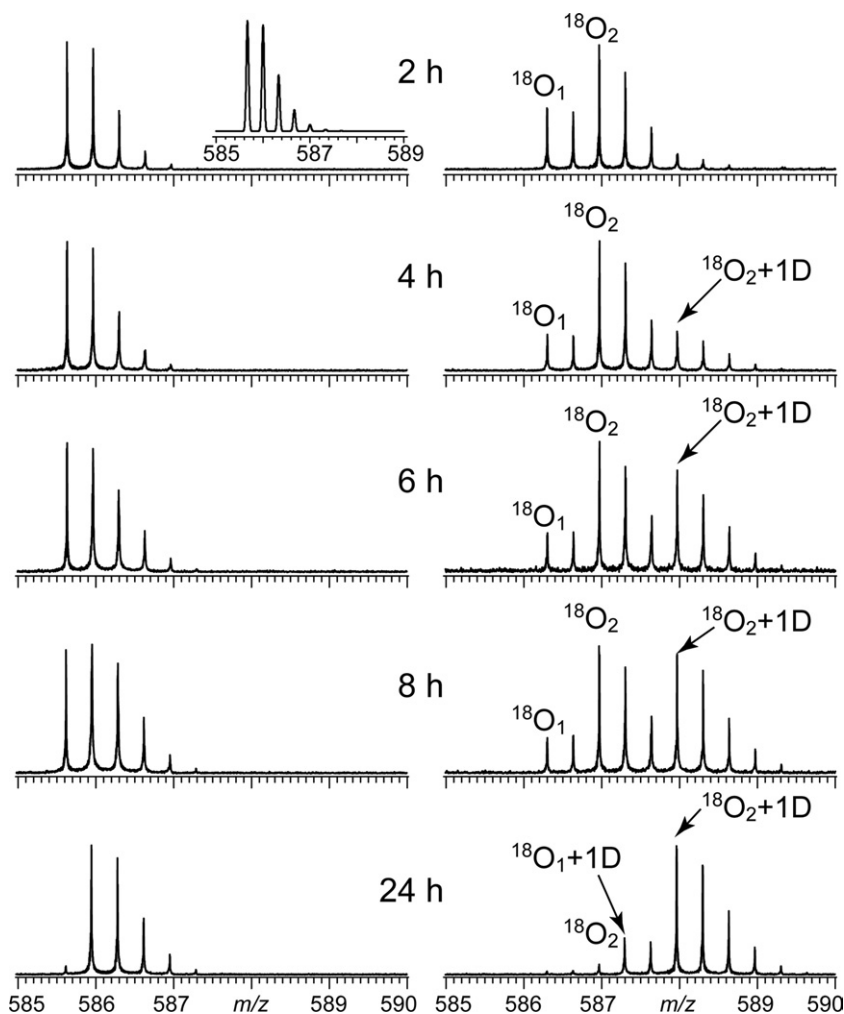


**Figure 1.** Mass spectra of the triply charged calmodulin peptide ( $^{91}VF\text{DKDNGYISAELR}_{106}$ ) extracted at different times from the tryptic digestion solution in  $H_2^{16}O$  (left column) and in  $H_2^{18}O$  (right column). The inset shows the theoretical isotopic distribution of this peptide. The isotopic clusters were assigned in the  $^{18}O$  spectra as  $^{18}O_m + nD$ , where  $m$  and  $n$  indicate the number of  $^{18}O$  incorporations and deamidations, respectively.

calcium concentration and regulates calcium-dependent enzymes [56]. A previous in vitro study found that the Asn97-Gly98 was the greatest contributor to the isoAsp formation in calmodulin [57].

In the control experiment performed in  $H_2^{16}O$ , there was an approximately 1-Da mass shift in the monoisotopic peak from the 2-h spectrum to the 24-h spectrum, indicating the onset of one deamidation in this peptide during the 24-h incubation period at 37 °C. The monoisotopic peak in the 2-h  $^{18}O$ -labeled spectrum showed a mass difference about 2 Da from that in the control spectrum, resulting from one  $^{18}O$  incorporation. The third isotopic peak had the highest intensity in the mass spectrum of this 2-h  $^{18}O$ -labeled peptide, and its mass was shifted by an additional approximately 2 Da, corresponding to a second  $^{18}O$  incorporation. The sixth isotopic peak became significant in the isotopic cluster in the 6-h spectrum, continued to increase in intensity in the 8-h spectrum, and became the most abundant peak

in the 24-h spectrum. This peak showed a mass shift of about 7 Da from the monoisotopic peak in the corresponding control spectrum, with the addition of about 4 Da coming from the double  $^{18}O$  substitution, and the remaining nearly 3 Da being the result of one deamidation occurring during the course of the tryptic digestion (Scheme 1). During the deamidation, the  $-NH_2$  group of the Asn residue was substituted by a hydroxyl group ( $-^{18}OH$ ) via the hydrolysis of the succinimide intermediate in  $H_2^{18}O$ , leading to an increase in the mass of a peptide by  $0.984 + 2.0043 = 2.988$  Da.

These results show that although deamidation readily occurred during a 24-h tryptic digestion of this easily deamidating calmodulin peptide (91–106), a short trypsin digestion ( $\sim 4$  h) would not introduce detectable deamidations. The first two  $^{18}O$  atoms were incorporated into this peptide's C-terminus, which will be further confirmed by the tandem MS experiment (see following text).



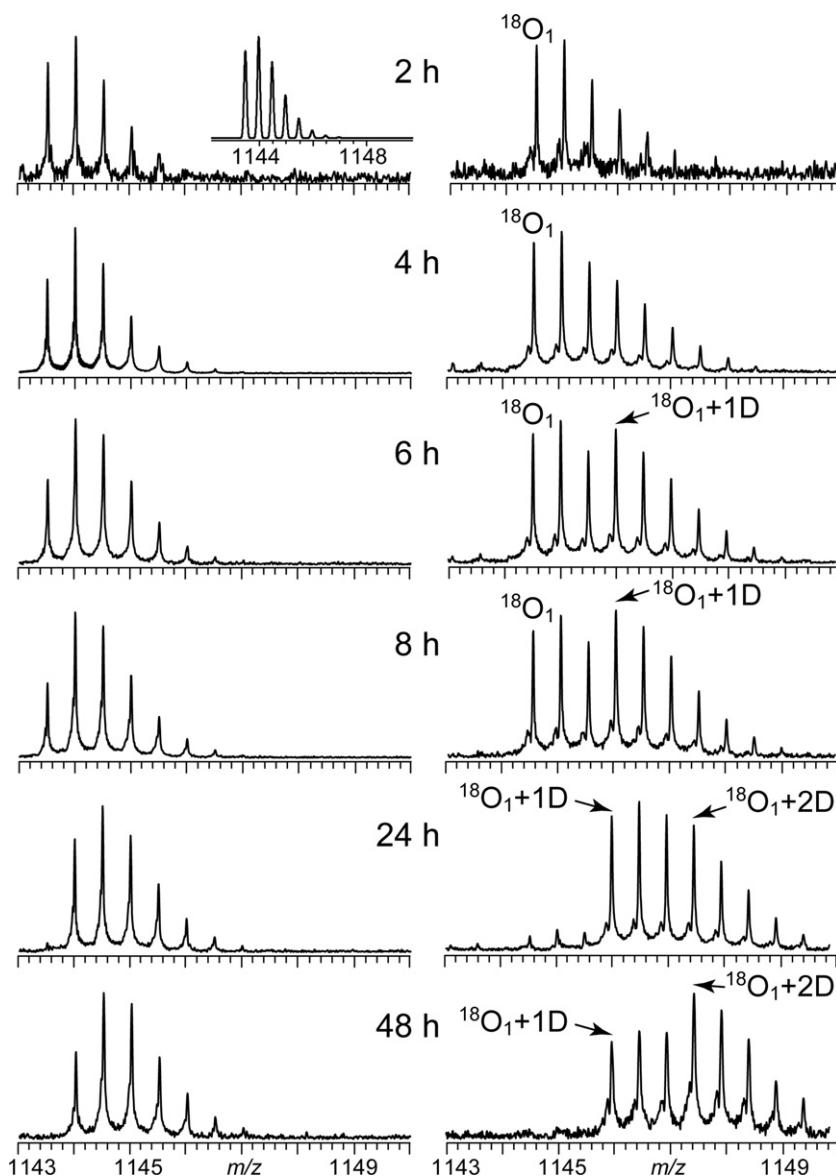


**Figure 2.** Mass spectra of the doubly charged RNase A peptide ( $^{67}\text{NGQTNC}^*\text{YQSYSTMSITDC}^*\text{R}_{85}$ ) extracted at different times from the tryptic digestion solution in  $\text{H}_2^{16}\text{O}$  (left column) and in  $\text{H}_2^{18}\text{O}$  (right column). The inset shows the theoretical isotopic distribution of this peptide. The isotopic clusters were assigned in the  $^{18}\text{O}$  spectra in the same way as in Figure 1.

### RNase A and Lysozyme Tryptic Peptides ESI FTMS Spectra ( $^{16}\text{O}$ versus $^{18}\text{O}$ )

Further experiments tested the trypsin digestion time course for tryptic peptides from RNase A (Figure 2) and lysozyme (Figure 3). Once again, the insets show the theoretical isotopic distributions of the corresponding peptides. The results from these time course studies are similar to the calmodulin tryptic peptide results in Figure 1, except that both of these peptides, which are also the most rapidly deamidating peptides from their respective proteins, contain two potential deamidation sites. Again, rapid digestion resulted in no detectable deamidation (<4 h for RNase A; <8 h for lysozyme) in these tryptic peptides. The RNase A tryptic peptide

showed little incorporation of a second  $^{18}\text{O}$  at the C-terminus, but demonstrated an abundant amount of double deamidation. The lysozyme tryptic peptide showed abundant double  $^{18}\text{O}$  substitutions at the C-terminus, but only one deamidation over the 48-h time course.

The RNase A tryptic peptide ( $^{67}\text{NGQTNC}^*\text{YQSYSTMSITDC}^*\text{R}_{85}$ ) contains the fast deamidating NG sequence at the N-terminus, near the exposed and flexible part of the peptide, where C\* denotes carbamidomethylated cysteine residue. There is little steric hindrance for the deamidation reaction, which may facilitate the succinimide intermediate formation and the hydrolysis in  $\text{H}_2^{18}\text{O}$ , thus making the deamidation

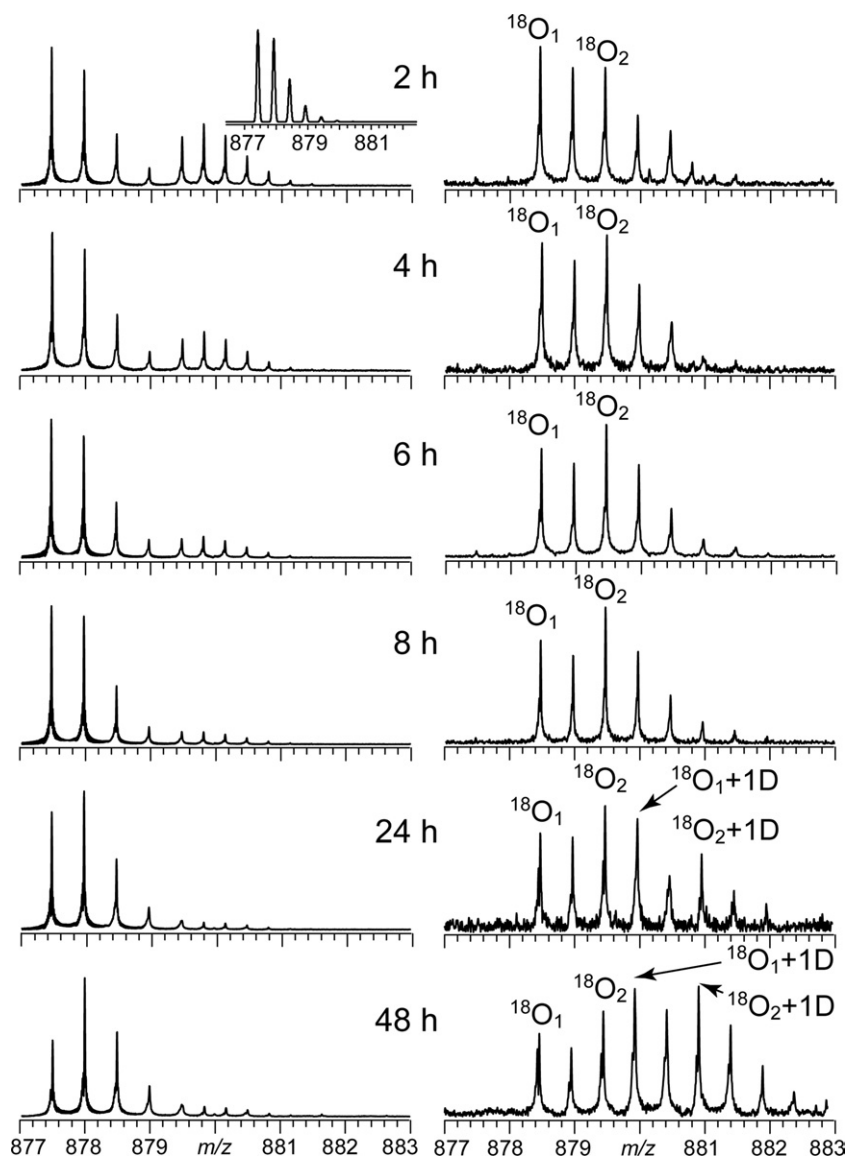


**Figure 3.** Mass spectra of the doubly charged lysozyme peptide ( $^{46}\text{NTDGSTDY}\text{GILQINSR}_{61}$ ) extracted at different times from the tryptic digestion solution in  $\text{H}_2^{16}\text{O}$  (left column) and in  $\text{H}_2^{18}\text{O}$  (right column). The inset shows the theoretical isotopic distribution of this peptide. The isotopic clusters were assigned in the  $^{18}\text{O}$  spectra in the same way as in Figure 1.

process even faster than the second  $^{18}\text{O}$  atom incorporation into the peptide C-terminus. The Thr located at the N-terminal side of the Asn71 residue is also known to accelerate deamidation [12], which may help to explain the second deamidation in this peptide. Moreover, deamidation in one site often causes protein conformational change and accelerates deamidation at a second site [5]. Since the TN is located near the N-terminal NG, a conformational change at the NG site will influence the TN local conformation, which may further contribute to the second site deamidation.

The lysozyme tryptic peptide ( $^{46}\text{NTDGSTDY}\text{GILQINSR}_{61}$ ) has the NT located at the N-terminus and the NS located near the C-terminus. The deamidation rate of this peptide was substantially slower than the calmodulin tryptic peptide and the RNase A tryptic pep-

ptide, evident from the control spectra. The one deamidation site of this lysozyme tryptic peptide is likely the Asn residue in the NS sequence for two reasons. First, a Ser residue following an Asn residue is known to promote Asn deamidation due to conformational flexibility and its polar side chain, which increases the deamidation rate compared to nonpolar groups [12]. Second, the NS is located near the C-terminus, which has little steric hindrance for nucleophilic attack. The assigned NS site deamidation also corroborates with the previous study, which found that the deamidation site at Asn59 of the lysozyme peptide Asp48 to Trp62 could be recognized by T cells, with a measured deamidation half-life of about 10 days in PBS buffer (pH 7.5) at 37 °C [1]. Unlike the NG and TN sites in the RNase A peptide, the NT and NS sites in this lysozyme tryptic

peptide are distant from each other so the conformational change induced by deamidation at one site may not have a substantial influence on the local conformation of the other. Finally, in all spectra of this lysozyme peptide, the major isotopic cluster was followed by another triply charged isotopic cluster, which was an unrelated tryptic peptide fragment residues (74–97). However, as evident from the control spectra, this second peptide was much less abundant than the peptide of interest in the 24- and 48-h samples, where appreciable deamidations were observed. Furthermore, in the <sup>18</sup>O-labeled spectra of samples taken after at least 6 h of digestion, there was no evidence for a triply charged peptide in the mass range of interest, which would have shown up in between adjacent isotopic peaks of the doubly charged peptide of interest due to its different charge state. Thus, its interference to the quantification of deamidation extent was expected to be minimal and no correction was attempted in the following analysis.

#### Quantification of the Extent of the <sup>18</sup>O Incorporation and Deamidation during the Digestion Time Course

The isotopic distribution in each <sup>18</sup>O-labeled peptide spectrum was deconvolved using the least-square fitting method. The initial values were obtained step by step, from the lightest isotopic cluster to the heaviest one. Using the 8-h calmodulin peptide spectrum as an example, the abundance of the <sup>18</sup>O<sub>1</sub> cluster was taken directly from the peak height of the first isotopic peak (A) and then its contribution (A + 2) to the third isotopic peak was calculated based on its theoretical isotopic distribution that, finally, was subtracted from the peak height of the third isotopic peak to give the abundance of the <sup>18</sup>O<sub>2</sub> cluster. This procedure was repeated until the abundances of all isotopic clusters were obtained. These initial abundance values were normalized to give the percentages, which were adjusted iteratively until the resulting sum of all isotopic distributions from the fitting gave the least sum-of-square deviations from the experimental distribution. The final percentages of all isotopic clusters as a function of digestion time were plotted in Figure 4a, b, and c for the calmodulin, RNase A, and lysozyme peptides, respectively. To test the variance of these abundances, triplicate experiments of the <sup>18</sup>O-labeled calmodulin tryptic peptide were done using the same method described earlier and the results are plotted in Figure 4d, which correlate well with the results from the single time experiment shown in Figure 4a. After the deconvolution, it was easier to follow the deamidation process taking place during the tryptic digestion in H<sub>2</sub><sup>18</sup>O. In general, the results agreed with those from the control experiment, showing that a short (4 h for the calmodulin RNase A peptides and 8 h for the lysozyme peptide) tryptic digestion would not introduce detectable artificial deamidations.

#### ECD of <sup>18</sup>O-Labeled Calmodulin Tryptic Peptide at Time Points 2 and 24 h

Figure 5 shows the ECD spectra of the 2- and 24-h time point samples from Figure 1. ECD is based on the dissociative recombination of multiply charged polypeptide molecules with low-energy electrons [58]. It cleaves the N–C<sub>α</sub> bond non-specifically and generates mostly c and z<sup>•</sup> ions, although its mechanism is still under debate [27–29].

The 2-h ECD spectrum showed c<sub>3</sub>–c<sub>15</sub> and z<sub>2</sub>–z<sub>14</sub><sup>•</sup> ions (Figure 5a). Neither c<sub>6</sub><sup>•</sup> + 58 nor z<sub>10</sub> – 57 ion was observed in this spectrum to indicate the deamidation of Asn97 to isoAsp. Although the [M – 60] fragment ion was observed (Figure 5a, inset), it most likely arose from the side-chain loss of the two pre-existing Asp residues (Asp93 and Asp95), since all c ions that contain the Asn97 residue (c<sub>7</sub> to c<sub>15</sub> ions) showed no +3-Da mass shift as one would expect if the Asn97 had deamidated in H<sub>2</sub><sup>18</sup>O. Furthermore, none of the c ions (particularly the c<sub>15</sub> ion) showed any mass shift compared with its normal counterpart produced in the control experiment (Supplementary Table 1), whereas all z<sup>•</sup> ions appeared to contain two adjacent isotopic clusters that were about 2 and 4 Da heavier than their <sup>16</sup>O counterparts. These results indicated that the first and second <sup>18</sup>O atoms were incorporated into the peptide's C-terminal carboxyl group, and no detectable deamidation occurred during the first 2 h of the tryptic digestion.

The 24-h ECD spectrum showed c<sub>3</sub>–c<sub>15</sub> ions and z<sub>2</sub>–z<sub>13</sub><sup>•</sup> ions (Figure 5b). As in the 2-h ECD spectrum, all z<sup>•</sup> ions contained two adjacent clusters of isotopic peaks, indicating one and two <sup>18</sup>O incorporations at the C-terminus. For z<sub>10</sub><sup>•</sup>–z<sub>13</sub><sup>•</sup> ions, both isotopic clusters were shifted in mass by an additional approximately 3 Da because they all included the Asn97 deamidation site. Although the c<sub>3</sub>–c<sub>6</sub> ions showed no mass shifts, the mass of c<sub>7</sub>–c<sub>15</sub> ions increased by about 3 Da when compared to their <sup>16</sup>O counterparts, once again indicative of the deamidation that occurred at the Asn97 residue (Supplementary Table 2). Moreover, both complementary diagnostic ions for the Asn97 deamidation to isoAsp, the c<sub>6</sub><sup>•</sup> + 60 and z<sub>10</sub> – 59 ions, were observed with nearly 1 ppm mass accuracy, with the 2-Da mass difference comparing with the normal diagnostic ions being the result of one <sup>18</sup>OH instead of one <sup>16</sup>OH substitution at the deamidation site (Figure 5b, insets). Like all other z<sup>•</sup> ions, the z<sub>10</sub> – 59 ion also had two isotopic clusters corresponding to one and two <sup>18</sup>O atom incorporations at the C-terminus. The [M(<sup>18</sup>O<sub>2</sub> + 1D) – 60] ion corresponding to the Asp side-chain loss was observed, as expected because of the two pre-existing Asp residues in this peptide. The side-chain loss peak of the Asp97 (as the result of Asn97 deamidation) should instead give rise to an [M(<sup>18</sup>O<sub>2</sub> + 1D) – 62] ion because of the <sup>18</sup>OH substitution at the deamidation site. Although this ion was indeed observed, it might

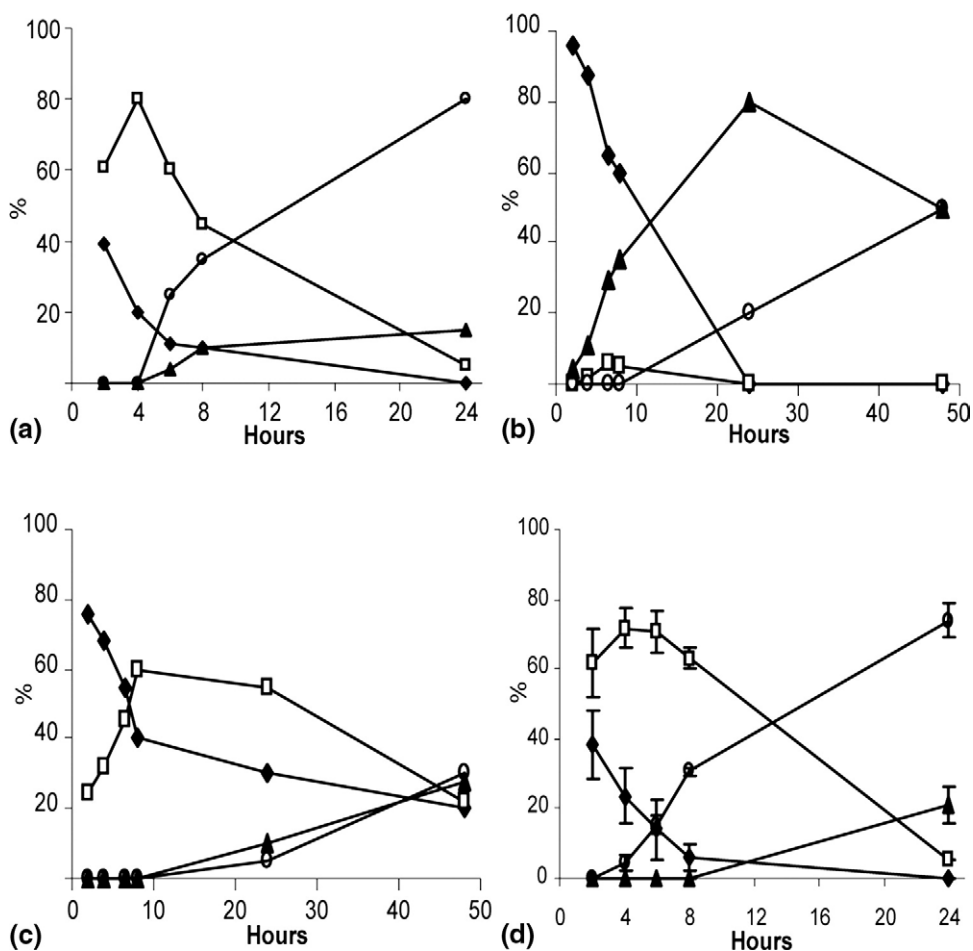


**Figure 4.** The percentage of each isotopic cluster at different digestion time as calculated using the least-squares method for the  $^{18}\text{O}$ -labeled: (a) calmodulin tryptic peptide (91–106), (b) RNase A tryptic peptide (67–85), (c) lysozyme tryptic peptide (46–61), and (d) calmodulin tryptic peptide (91–106) triplicate experiments. (a–d) —◆—:  $^{18}\text{O}_1$ , —□—:  $^{18}\text{O}_2$ , —▲—:  $^{18}\text{O}_1 + 1\text{D}$ , —○—:  $^{18}\text{O}_2 + 1\text{D}$ , except in (b)  $^{18}\text{O}_1 + 2\text{D}$ .

also come from the normal Asp side-chain loss of the singly  $^{18}\text{O}$ -labeled molecular ion that consisted of a significant portion of the total molecular ion population (Figure 4a, d); that is, it was actually an  $[\text{M}(^{18}\text{O}_1 + 1\text{D}) - 60]$  ion. The best evidence for the Asp formation from the Asn97 deamidation was perhaps the observation of an isotopic peak at another approximately 2 Da lighter than the  $[\text{M}(^{18}\text{O}_1 + 1\text{D}) - 60]$  peak (Figure 5b, inset, marked by the number sign, #), which could only be the  $[\text{M}(^{18}\text{O}_1 + 1\text{D}) - 62]$  ion, since there was little  $[\text{M}(^{18}\text{O}_0 + 1\text{D})]$  in the 24-h sample (bottom right spectrum, Figure 1). The detailed peak lists for the ECD experiments are available in the supplementary data (Supplementary Tables 1 and 2).

### Influencing Factors

There are several factors that can significantly affect the accuracy of the  $^{18}\text{O}$ -labeling experiment. First, formic acid should not be used to halt the digestion

reaction [49]. Apparently the acidic environment influenced the  $^{18}\text{O}$  incorporation and the  $^{18}\text{O}$ -labeling ratio (data not shown). Second, only  $\text{H}_2^{18}\text{O}$  should be used in the desalting step. If  $\text{H}_2^{16}\text{O}$  was instead used in this step, the  $^{18}\text{O}$  atom that had already been incorporated into the tryptic peptides might be exchanged by the  $^{16}\text{O}$  atom in the solvent, which would influence the accuracy of the  $^{18}\text{O}$  incorporation measurement (data not shown). Centrifugation under vacuum appeared to further accelerate the back exchange with  $\text{H}_2^{16}\text{O}$ . Finally, excessive desalting should also be avoided. If  $\text{H}_2^{18}\text{O}$  was used more than three times to wash out the salts, it could also distort the  $^{18}\text{O}$  incorporation ratio (data not shown).

### Conclusions

During trypsin digestion, the deamidation rate of the released peptides increases, which may introduce unwanted artificial deamidation that is of no biological relevance. This paper demonstrated the use of



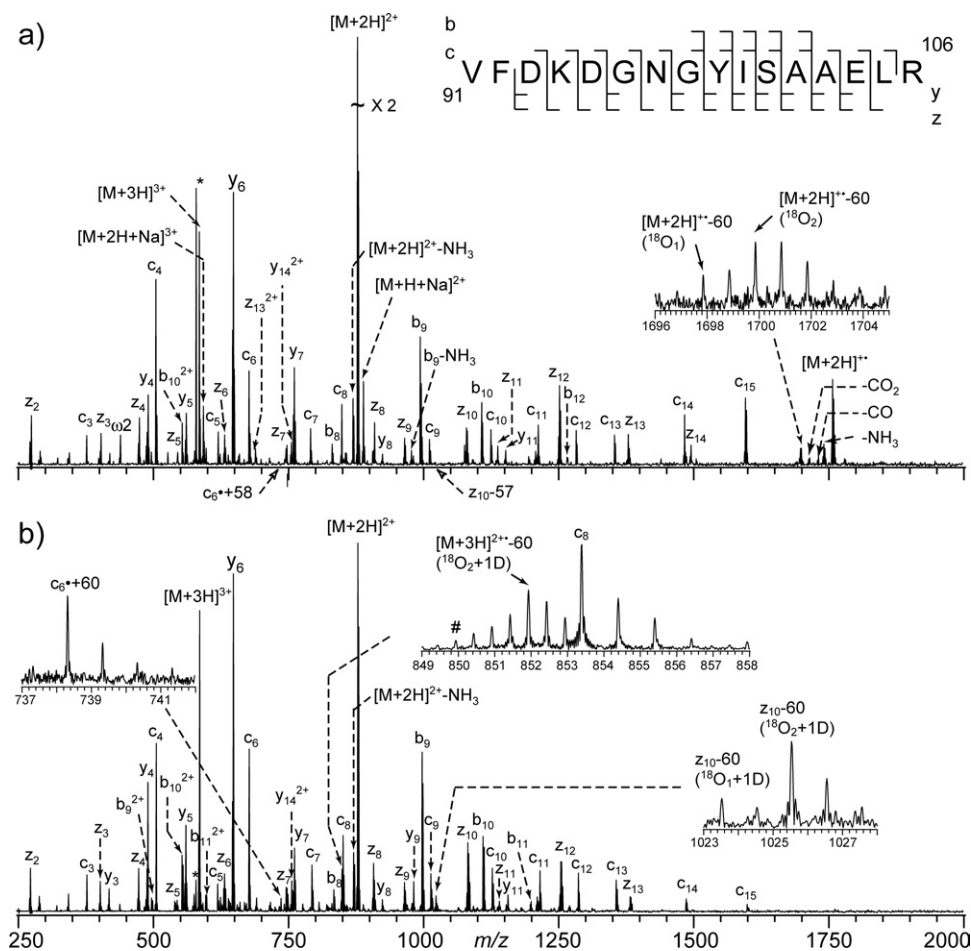


**Figure 5.** ECD spectra of the triply charged calmodulin tryptic peptide (91–106) labeled in  $\text{H}_2^{18}\text{O}$  at different time points: (a) 2 h, (b) 24 h. The insets of (a) show the  $[M - 60]$  ion and the cleavage pattern. The insets of (b) show the isotopic distributions of the  $c_6 + 60$  (left),  $[M - 60]$  (middle), and  $z_{10} - 59$  (right) ions. \*: electronic noise,  $\omega 2$ : harmonics.

$\text{H}_2^{18}\text{O}$  as a mass labeling reagent during the trypsin digestion process to distinguish between the deamidation that occurred during sample handling procedures (+3 Da mass increases) and the deamidation that was native to the sample (+1 Da). Tandem mass methods, such as ECD, can further help locate the sites of deamidation and  $^{18}\text{O}$  incorporation. The use of  $^{18}\text{O}$ , however, generated complex isotopic patterns that must be deconvolved first. In addition, care must be taken so that the isotopic distributions would not be distorted artificially during the digestion, centrifugation, and desalting steps. This study showed that fast trypsin digestion ( $\sim 4$  h) generally would not introduce additional detectable deamidations, even for the most rapidly deamidating peptides studied here. This result should increase the confidence in the quantification of Asn, Asp, and isoAsp residues, when samples need to be digested first to small peptides to facilitate the mass spectrometry analysis. Finally, this  $^{18}\text{O}$ -labeling methodology can be easily extended to study the artificial deamidation taking place in other protein sample preparation procedures.

## Acknowledgments

The authors gratefully acknowledge the financial support from the NIH/NCRR P41RR10888, NIH/NHLBI N01HV28178, NIH/NIGMS R01GM078293, MSD SCIEX, and the ACS Petroleum Research Fund. The authors also thank Raman Mathur, Dr. Vera B. Ivleva, Dr. Cheng Zhao, Dr. Chunxiang Yao, Konstantine Aizikov, and Nadezda Sargaeva for helpful discussions.

## References

- Robinson, N. E.; Robinson, A. B. *Molecular Clocks: Deamidation of Asparaginyl and Glutaminyl Residues in Peptides and Proteins*. Althouse Press: Cave Junction, OR, 2004.
- Robinson, N. E. Protein Deamidation. *Proc. Natl. Acad. Sci. U. S. A.* **2002**, *99*, 5283–5288.
- Robinson, N. E.; Robinson, A. B. Molecular Clocks. *Proc. Natl. Acad. Sci. U. S. A.* **2001**, *98*, 944–949.
- Lindner, H.; Sarg, B.; Hoertnagl, B.; Helliger, W. The Microheterogeneity of the Mammalian H1(0) Histone—Evidence for an Age-Dependent Deamidation. *J. Biol. Chem.* **1998**, *273*, 13324–13330.
- Bischoff, R.; Kolbe, H. V. Deamidation of Asparagine and Glutamine Residues in Proteins and Peptides—Structural Determinants and Analytical Methodology. *J. Chromatogr. B Biomed. Appl.* **1994**, *662*, 261–278.
- Lindner, H.; Helliger, W. Age-Dependent Deamidation of Asparagine Residues in Proteins. *Exp. Gerontol.* **2001**, *36*, 1551–1563.
- Capasso, S. Estimation of the Deamidation Rate of Asparagine Side Chains. *J. Pept. Res.* **2000**, *55*, 224–229.

8. Geiger, T.; Clarke, S. Deamidation, Isomerization, and Racemization at Asparaginyl and Aspartyl Residues in Peptides—Succinimide-Linked Reactions That Contribute to Protein-Degradation. *J. Biol. Chem.* **1987**, *262*, 785–794.
9. Xie, M. L.; Schowen, R. L. Secondary Structure and Protein Deamidation. *J. Pharm. Sci.* **1999**, *88*, 8–13.
10. Robinson, N. E.; Robinson, A. B. Prediction of Protein Deamidation Rates from Primary and Three-Dimensional Structure. *Proc. Natl. Acad. Sci. U. S. A.* **2001**, *98*, 4367–4372.
11. Tylercross, R.; Schirch, V. Effects of Amino-Acid-Sequence, Buffers, and Ionic-Strength on the Rate and Mechanism of Deamidation of Asparagine Residues in Small Peptides. *J. Biol. Chem.* **1991**, *266*, 22549–22556.
12. Wright, H. T. Nonenzymatic Deamidation of Asparaginyl and Glutaminyl Residues in Proteins. *Crit. Rev. Biochem. Mol. Biol.* **1991**, *26*, 1–52.
13. Kossiakoff, A. A. Tertiary Structure Is a Principal Determinant to Protein Deamidation. *Science* **1988**, *240*, 191–194.
14. Peters, B.; Trout, B. L. Asparagine Deamidation: pH-Dependent Mechanism from Density Functional Theory. *Biochemistry* **2006**, *45*, 5384–5392.
15. Joshi, A. B.; Sawai, M.; Kearney, W. R.; Kirsch, L. E. Studies on the Mechanism of Aspartic Acid Cleavage and Glutamine Deamidation in the Acidic Degradation of Glucagon. *J. Pharm. Sci.* **2005**, *94*, 1912–1927.
16. Robinson, N. E.; Zabrowskov, V.; Zhang, J.; Lampi, K. J.; Robinson, A. B. Measurement of Deamidation of Intact Proteins by Isotopic Envelope and Mass Defect with Ion Cyclotron Resonance Fourier Transform Mass Spectrometry. *Rapid Commun. Mass Spectrom.* **2006**, *20*, 3535–3541.
17. Robinson, N. E.; Lampi, K. J.; Speir, J. P.; Kruppa, G.; Easterling, M.; Robinson, A. B. Quantitative Measurement of Young Human Eye Lens Crystallins by Direct Injection Fourier Transform Ion Cyclotron Resonance Mass Spectrometry. *Mol. Vis.* **2006**, *12*, 704–711.
18. Robinson, N. E.; Lampi, K. J.; McIver, R. T.; Williams, R. H.; Muster, W. C.; Kruppa, G.; Robinson, A. B. Quantitative Measurement of Deamidation in Lens Beta B2-Crystallin and Peptides by Direct Electrospray Injection and Fragmentation in a Fourier Transform Mass Spectrometer. *Mol. Vis.* **2005**, *11*, 1211–1219.
19. Schmid, D. G.; von der Mulbe, F.; Fleckenstein, B.; Weinschenk, T.; Jung, G. Broadband Detection Electrospray Ionization Fourier Transform Ion Cyclotron Resonance Mass Spectrometry to Reveal Enzymatically and Chemically Induced Deamidation Reactions within Peptides. *Anal. Chem.* **2001**, *73*, 6008–6013.
20. Chazin, W. J.; Kordel, J.; Thulin, E.; Hofmann, T.; Drakenberg, T.; Forsen, S. Identification of an Isoaspartyl Linkage Formed upon Deamidation of Bovine Calbindin-D<sub>9k</sub> and Structural Characterization by 2D <sup>1</sup>H NMR. *Biochemistry* **1989**, *28*, 8646–8653.
21. Carlson, A. D.; Riggan, R. M. Development of Improved High-Performance Liquid Chromatography Conditions for Nonisotopic Detection of Isoaspartic Acid to Determine the Extent of Protein Deamidation. *Anal. Biochem.* **2000**, *278*, 150–155.
22. Carr, S. A.; Hemling, M. E.; Bean, M. F.; Roberts, G. D. Integration of Mass-Spectrometry in Analytical Biotechnology. *Anal. Chem.* **1991**, *63*, 2802–2824.
23. Zhang, W.; Czupryn, M. J. Analysis of Isoaspartate in a Recombinant Monoclonal Antibody and Its Charge Isoforms. *J. Pharm. Biomed. Anal.* **2003**, *30*, 1479–1490.
24. Gonzalez, L. J.; Shimizu, T.; Satomi, Y.; Betancourt, L.; Besada, V.; Padron, G.; Orlando, R.; Shirasawa, T.; Shimonishi, Y.; Takao, T. Differentiating Alpha- and Beta-Aspartic Acids by Electrospray Ionization and Low-Energy Tandem Mass Spectrometry. *Rapid Commun. Mass Spectrom.* **2000**, *14*, 2092–2102.
25. Castet, S.; Enjalbal, C.; Fulcrand, P.; Guichou, J. F.; Martinez, J.; Aubagnac, J. L. Characterization of Aspartic Acid and Beta-Aspartic Acid in Peptides by Fast-Atom Bombardment Mass Spectrometry and Tandem Mass Spectrometry. *Rapid Commun. Mass Spectrom.* **1996**, *10*, 1934–1938.
26. Zubarev, R. A.; Kelleher, N. L.; McLafferty, F. W. Electron Capture Dissociation of Multiply Charged Protein Cations. A Nonergodic Process. *J. Am. Chem. Soc.* **1998**, *120*, 3265–3266.
27. Zubarev, R. A.; Haselmann, K. F.; Budnik, B.; Kjeldsen, F.; Jensen, F. Towards an Understanding of the Mechanism of Electron-Capture Dissociation: A Historical Perspective and Modern Ideas. *Eur. J. Mass Spectrom.* **2002**, *8*, 337–349.
28. Syrstad, E. A.; Turecek, F. Toward a General Mechanism of Electron Capture Dissociation. *J. Am. Soc. Mass Spectrom.* **2005**, *16*, 208–224.
29. Leymarie, N.; Costello, C. E.; O'Connor, P. B. Electron Capture Dissociation Initiates a Free Radical Reaction Cascade. *J. Am. Chem. Soc.* **2003**, *125*, 8949–8958.
30. Coon, J. J.; Syka, J. E. P.; Schwartz, J. C.; Shabanowitz, J.; Hunt, D. F. Anion Dependence in the Partitioning between Proton and Electron Transfer in Ion/Ion Reactions. *Int. J. Mass Spectrom.* **2004**, *236*, 33–42.
31. Syka, J. E. P.; Coon, J. J.; Schroeder, M. J.; Shabanowitz, J.; Hunt, D. F. Peptide and Protein Sequence Analysis by Electron Transfer Dissociation Mass Spectrometry. *Proc. Natl. Acad. Sci. U. S. A.* **2004**, *101*, 9528–9533.
32. Cournoyer, J. J.; Lin, C.; Bowman, M. J.; O'Connor, P. B. Quantitating the Relative Abundance of Isoaspartyl Residues in Deamidated Proteins by Electron Capture Dissociation. *J. Am. Soc. Mass Spectrom.* **2007**, *18*, 48–56.
33. Cournoyer, J. J.; Lin, C.; O'Connor, P. B. Detecting Deamidation Products in Proteins by Electron Capture Dissociation. *Anal. Chem.* **2006**, *78*, 1264–1271.
34. Cournoyer, J. J.; Pittman, J. L.; Ivleva, V. B.; Fallows, E.; Waskell, L.; Costello, C. E.; O'Connor, P. B. Deamidation: Differentiation of Aspartyl from Isoaspartyl Products in Peptides by Electron Capture Dissociation. *Protein Sci.* **2005**, *14*, 452–463.
35. O'Connor, P. B.; Cournoyer, J. J.; Pitteri, S. J.; Chrisman, P. A.; McLuckey, S. A. Differentiation of Aspartic and Isoaspartic Acids Using Electron Transfer Dissociation. *J. Am. Soc. Mass Spectrom.* **2006**, *17*, 15–19.
36. Horn, D. M.; Ge, Y.; McLafferty, F. W. Activated Ion Electron Capture Dissociation for Mass Spectral Sequencing of Larger (42 kDa) Proteins. *Anal. Chem.* **2000**, *72*, 4778–4784.
37. Yao, X. D.; Freas, A.; Ramirez, J.; Demirev, P. A.; Fenselau, C. Proteolytic O-18 Labeling for Comparative Proteomics: Model Studies with Two Serotypes of Adenovirus. *Anal. Chem.* **2004**, *76*, 2675–2675.
38. Stewart, I. I.; Thomson, T.; Figeys, D. O-18 Labeling: A Tool for Proteomics. *Rapid Commun. Mass Spectrom.* **2001**, *15*, 2456–2465.
39. Heller, M.; Mattou, H.; Menzel, C.; Yao, X. D. Trypsin Catalyzed O-16-to-O-18 Exchange for Comparative Proteomics: Tandem Mass Spectrometry Comparison Using MALDI-TOF, ESI-QTOF, and ESI-Ion Trap Mass Spectrometers. *J. Am. Soc. Mass Spectrom.* **2003**, *14*, 704–718.
40. Yao, X. D.; Freas, A.; Ramirez, J.; Demirev, P. A.; Fenselau, C. Proteolytic O-18 Labeling for Comparative Proteomics: Model Studies with Two Serotypes of Adenovirus. *Anal. Chem.* **2001**, *73*, 2836–2842.
41. Miyagi, M.; Rao, K. C. S. Proteolytic O-18-Labeling Strategies for Quantitative Proteomics. *Mass Spectrom. Rev.* **2007**, *26*, 121–136.
42. Katta, V.; Chait, B. T. Hydrogen/Deuterium Exchange Electrospray Ionization Mass Spectrometry: A Method for Probing Protein Conformational Changes in Solution. *J. Am. Chem. Soc.* **1993**, *115*, 6317–6321.
43. Wales, T. E.; Engen, J. R. Hydrogen Exchange Mass Spectrometry for the Analysis of Protein Dynamics. *Mass Spectrom. Rev.* **2006**, *25*, 158–170.
44. Garcia, R. A.; Pantazatos, D.; Villarreal, F. J. Hydrogen/Deuterium Exchange Mass Spectrometry for Investigating Protein-Ligand Interactions. *Assay Drug. Dev. Technol.* **2004**, *2*, 81–91.
45. Kheterpal, I.; Cook, K. D.; Wetzel, R. Hydrogen/Deuterium Exchange Mass Spectrometry Analysis of Protein Aggregates. *Methods Enzymol.* **2006**, *413*, 140–166.
46. Kheterpal, I.; Wetzel, R. Hydrogen/Deuterium Exchange Mass Spectrometry—A Window into Amyloid Structure. *Acc. Chem. Res.* **2006**, *39*, 584–593.
47. Xiao, G.; Bondarenko, P. V.; Jacob, J.; Chu, G. C.; Chelius, D. O18 Labeling Method for Identification and Quantification of Succinimide in Proteins. *Anal. Chem.* **2007**, *79*, 2714–2721.
48. Kubota, K.; Yoneyama-Takazawa, T.; Ichikawa, K. Determination of Sites Citrullinated by Peptidylarginine Deiminase Using O-18 Stable Isotope Labeling and Mass Spectrometry. *Rapid Commun. Mass Spectrom.* **2005**, *19*, 683–688.
49. Schnolzer, M.; Jedrzejewski, P.; Lehmann, W. D. Protease-Catalyzed Incorporation of O-18 into Peptide Fragments and Its Application for Protein Sequencing by Electrospray and Matrix-Assisted Laser Desorption/Ionization Mass Spectrometry. *Electrophoresis* **1996**, *17*, 945–953.
50. Antonov, V. K.; Ginodman, L. M.; Rumsh, L. D.; Kapitannikov, Y. V.; Barshevskaya, T. N.; Yavashchev, L. P.; Gurova, A. G.; Volkova, L. I. Studies on the Mechanisms of Action of Proteolytic Enzymes Using Heavy Oxygen Exchange. *Eur. J. Biochem.* **1981**, *117*, 195–200.
51. O'Connor, P. B.; Pittman, J. L.; Thomson, B. A.; Budnik, B. A.; Cournoyer, J. C.; Jebanathirajah, J.; Lin, C.; Moyer, S.; Zhao, C. A New Hybrid Electrospray Fourier Transform Mass Spectrometer: Design and Performance Characteristics. *Rapid Commun. Mass Spectrom.* **2006**, *20*, 259–266.
52. Jebanathirajah, J. A.; Pittman, J. L.; Thomson, B. A.; Budnik, B. A.; Kaur, P.; Rape, M.; Kirschner, M.; Costello, C. E.; O'Connor, P. B. Characterization of a New qQq-FTICR Mass Spectrometer for Post-translational Modification Analysis and Top-Down Tandem Mass Spectrometry of Whole Proteins. *J. Am. Soc. Mass Spectrom.* **2005**, *16*, 1985–1999.
53. Tsybin, Y. O.; Witt, M.; Baykut, G.; Hakansson, P. Electron Capture Dissociation Fourier Transform Ion Cyclotron Resonance Mass Spectrometry in the Electron Energy Range 0–50 eV. *Rapid Commun. Mass Spectrom.* **2004**, *18*, 1607–1613.
54. Tsybin, Y. O.; Hakansson, P.; Budnik, B. A.; Haselmann, K. F.; Kjeldsen, F.; Gorskov, M.; Zubarev, R. A. Improved Low-Energy Electron Injection Systems for High Rate Electron Capture Dissociation in Fourier Transform Ion Cyclotron Resonance Mass Spectrometry. *Rapid Commun. Mass Spectrom.* **2001**, *15*, 1849–1854.
55. Tsybin, Y. O.; Ramstrom, M.; Witt, M.; Baykut, G.; Hakansson, P. Peptide and Protein Characterization by High-Rate Electron Capture Dissociation Fourier Transform Ion Cyclotron Resonance Mass Spectrometry. *J. Mass Spectrom.* **2004**, *39*, 719–729.
56. Cheung, W. Y. Calmodulin Plays a Pivotal Role in Cellular Regulation. *Science* **1980**, *207*, 19–27.
57. Potter, S. M.; Henzel, W. J.; Aswad, D. W. In-Vitro Aging of Calmodulin Generates Isoaspartate at Multiple Asn-Gly and Asp-Gly Sites in Calcium-Binding Domains II, III, and IV. *Protein Sci.* **1993**, *2*, 1648–1663.
58. Zubarev, R. A. Electron-Capture Dissociation Tandem Mass Spectrometry. *Curr. Opin. Biotechnol.* **2004**, *15*, 12–16.
59. Yergey, J. A. A general approach to calculating isotopic distributions for mass spectrometry. *Int. J. Mass Spectrom. Ion Processes* **1983**, *52*, 337–349.